

**THE BOND BEHAVIOR OF INDIGENOUSLY
MANUFACTURED GLASS FIBER
REINFORCED POLYMER BARS**

By

Imran Raza Jafri

(2004 – NUST – MS PhD – STR – 07)

A Thesis submitted in partial fulfillment of
the requirements for the degree of
Master of Science

In

Department of Civil Engineering

National Institute of Transportation

National University of Sciences and Technology

Rawalpindi, Pakistan

(2006)

This is to certify that the

thesis titled

**THE BOND BEHAVIOR OF INDIGENOUSLY
MANUFACTURED GLASS FIBER
REINFORCED POLYMER BARS**

Submitted by

Imran Raza Jafri

Has been accepted towards the partial fulfillment

of

the requirements

for

Master of Science in Civil Engineering

Brigadier Dr. Tayyeb Akram, PhD (USA)

National Institute of Transportation, Risalpur

National University of Sciences and Technology, Rawalpindi

**THE BOND BEHAVIOR OF INDIGENOUSLY
MANUFACTURED GLASS FIBER
REINFORCED POLYMER BARS**

By

Imran Raza Jafri

A Thesis

of

Master of Science

Submitted to the

National Institute of Transportation

Risalpur

National University of Sciences and Technology

Rawalpindi

In partial fulfillment of the requirements

For the degree of

Master of Science in Civil Engineering

2006

DEDICATED
TO
MY PARENTS AND FAMILY

ACKNOWLEDGEMENT

I am thankful to All Mighty Allah, who gave me strength and patience to complete my research.

I would like to extent my wholehearted gratitude and appreciations to Dr. Tayyab Akram, Advisor and Committee Chairman, for providing innumerable inspiration and invaluable support to me in the completion of my research work. I am also thankful to committee members, Lieutenant Colonel Shabbir Ahmad, Lecturer Shaukat Ali Khan, and Lecturer Shazim Ali Memon for their incalculable advice and guidance in concluding my thesis.

I would like to specially thank Mr. Mahmood Khalid, CEO, Fiber Craft Industries, Harbanspura Lahore, with out whose cooperation this project could never have been completed.

In the end, I pay my earnest gratitude with sincere sense of respect to my parents, and family for their unending support, encouragement, prayers and patience.

ABSTRACT

There is trend of using Fiber Reinforced Polymer (FRP) rods as reinforcing bars in reinforced concrete. This type of rebar provides a solution to the problem of durability of ordinary steel bars in reinforced concrete, which do not exhibit adequate corrosion resistance in a severe environment. FRP rebars exhibit good mechanical and corrosion resistance properties in severe conditions.

Bond development is one of the main behavioral aspects of reinforced concrete structures. Tests by previous researchers have shown that the bond behavior of FRP rebars is different from that of steel rebars and also varies with the type FRP rebar material. There is need to develop better understanding of bond behavior in FRP rebars.

In this research results from pullout bond tests performed on commercially available Glass Fiber-Reinforced Polymer (GFRP) rebars manufactured in Pakistan are presented and discussed. The study evaluates the influence of various parameters that affect bond strength and development such as the embedment length, surface characteristics, and diameter of the bar as well as concrete strength.

The results indicate that the spirally wrapped deformed GRFP rebars perform well in bond behavior. The concrete strength has no effect on bond strength, and the bond strength reduces with increase in GFRP rebar diameter and embedment length.

TABLE OF CONTENTS

CHAPTER		PAGE
1	INTRODUCTION	1
	1.1 GENERAL BACK GROUND	1
	1.2 PROBLEM STATEMENT	2
	1.3 SCOPE	2
	1.4 OBJECTIVES	3
2	LITERATURE REVIEW	4
	2.1 GENERAL	4
	2.2 GFRP MATERIALS	5
	2.2.1 Properties of GFRP Rebars	5
	2.2.2 GFRP Manufacturing Process	5
	2.3 FRP BOND BEHAVIOR	5
	2.3.1 Comparison of Steel and GFRP Bond Behavior	6
	2.3.2 Influence of Embedment Length on Bond Strength	6
	2.3.3 Influence of Compressive Strength on Bond Strength	7
	2.3.4 Influence of FRP Rebar Diameter on Bond Strength	7
	2.3.5 Influence of Surface Texture on Bond Strength	7
3	EXPERIMENTAL INVESTIGATION	9
	3.1 GENERAL	9
	3.2 ESTABLISHMENT OF VARIABLES	9
	3.3 MATERIAL PROPERTIES	9
	3.3.1 Concrete properties	9
	3.3.2 Glass Fiber Reinforced Polymer (GFRP) Rebar Properties	10
	3.4 SPECIMENS DESIGNATION	11

3.5	PREPARATION AND CASTING OF SPECIMENS	12
3.6	TESTING OF SPECIMENS	14
4	TEST RESULTS AND ANALYSIS	16
4.1	BOND STRESS VERSUS SLIP OF GFRP REBAR	16
4.1.1	Deformed GFRP Rebars	16
4.1.2	Sand Coated GFRP Rebars	17
4.1.3	Plain GFRP Rebars	17
4.2	BOND FAILURE MODE OF GFRP REBARS	17
4.3	FACTORS INFLUENCING BOND BEHAVIOR OF GFRP REBARS	19
4.3.1	Embedment Length	19
4.3.2	Bar Size	21
4.3.3	Surface Deformations	22
4.3.4	Concrete Strength	22
5	CONCLUSIONS AND RECOMMENDATIONS	24
5.1	CONCLUSIONS	24
5.2	RECOMMENDATIONS	24
	APPENDIX I	25
	REFERENCES	62

LIST OF FIGURES

FIGURE	TITLE	PAGE
2.1	GFRP rebars of various diameters and surface types	8
3.1	GFRP rebars cast in concrete cubes with bar alignment jig	13
3.2	Schematic details of pullout bond test	15
4.1	Damage to the deformed GFRP bar after pullout	18
4.2	Sand coated GFRP rebar, sand coating completely peeled off after test	18
4.3	Cross-section of concrete block showing crushed resin and chopped glass fiber remains	19
4.4	Influence of embedment length on maximum bond stress #4 deformed GFRP rebar	20
4.5	Influence of embedment length on maximum bond stress #3 deformed GFRP rebar	20
4.6	Influence of embedment length on maximum bond stress #2 deformed rebar	21
4.7	Influence of rebar diameter on maximum bond stress	21
4.8	Effect of surface texture deformation and embedment length on maximum bond stress	22
4.9	Influence of concrete compressive strength on bond stress of #3 deformed rebars	23
I.1	Bond slip curve for B2-D-3-3d-2	40
I.2	Bond slip curve for B2-D-4-3d-1	40
I.3	Bond slip curve for B2-D-4-3d-2	41
I.4	Bond slip curve for B3-D-2-3d-2	41
I.5	Bond slip curve for B4-D-4-3d-1	42
I.6	Bond slip curve for B4-D-4-3d-2	42
I.7	Bond slip curve for B6-D-3-3d-1	43
I.8	Bond slip curve for B6-D-3-3d-2	43
I.9	Bond slip curve for B7-D-3-3d-1	44
I.10	Bond slip curve for B7-D-3-3d-2	44

I.11	Bond slip curve for B8-D-4-3d-1	45
I.12	Bond slip curve for B8-D-4-3d-2	45
I.13	Bond slip curve for B9-D-2-3d-2	46
I.14	Bond slip curve for B10-D-4-7d-1	46
I.15	Bond slip curve for B10-D-4-5d-1	47
I.16	Bond slip curve for B11-D-3-7d-1	47
I.17	Bond slip curve for B11-D-3-5d-1	48
I.18	Bond slip curve for B12-D-2-7d-1	48
I.19	Bond slip curve for B12-D-2-5d-1	49
I.20	Bond slip curve for B1-SC-4-3d-1	49
I.21	Bond slip curve for B1-SC-3-3d-1	50
I.22	Bond slip curve for B1-SC-4-3d-2	50
I.23	Bond slip curve for B3-SC-2-3d-1	51
I.24	Bond slip curve for B4-SC-4-3d-1	51
I.25	Bond slip curve for B4-SC-4-3d-2	52
I.26	Bond slip curve for B5-SC-2-3d-2	52
I.27	Bond slip curve for B6-SC-3-3d-1	53
I.28	Bond slip curve for B6-SC-3-3d-2	53
I.29	Bond slip curve for B7-SC-3-3d-1	54
I.30	Bond slip curve for B7-SC-3-3d-2	54
I.31	Bond slip curve for B8-SC-4-3d-1	55
I.32	Bond slip curve for B8-SC-4-3d-2	55
I.33	Bond slip curve for B9-SC-2-3d-1	56
I.34	Bond slip curve for B9-SC-2-3d-2	56
I.35	Bond slip curve for B10-SC-4-5d-1	57
I.36	Bond slip curve for B11-SC-3-7d-1	57
I.37	Bond slip curve for B11-SC-3-5d-1	58
I.38	Bond slip curve for B12-SC-2-5d-1	58
I.39	Bond slip curve for B4-P-4-3d-1	59
I.40	Bond slip curve for B4-P-4-3d-2	59
I.41	Bond slip curve for B6-P-3-3d-1	60
I.42	Bond slip curve for B10-P-4-7d-1	60

I.43	Bond slip curve for B10-P-4-5d-1	61
I.44	Bond slip curve for B11-P-3-7d-1	61

LIST OF TABLES

TABLE	TITLE	PAGE
3.1	Compressive Strength of Concrete Cubes at 28 Days	10
3.2	Types of Bars Used in Pullout Tests	11
3.3	Specimen Designation Symbols	11
3.4	Schedule for the Casting of Pullout Specimens	13
I.1	Experimental Results	25
I.2	Test Data for Specimen B2-D-3-3d-2	27
I.3	Test Data for Specimen B2-D-4-3d-1	27
I.4	Test Data for Specimen B2-D-4-3d-2	27
I.5	Test Data for Specimen B3-D-2-3d-2	27
I.6	Test Data for Specimen B4-D-4-3d-1	28
I.7	Test Data for Specimen B4-D-4-3d-2	28
I.8	Test Data for Specimen B6-D-3-3d-1	28
I.9	Test Data for Specimen B6-D-3-3d-2	29
I.10	Test Data for Specimen B7-D-3-3d-1	29
I.11	Test Data for Specimen B7-D-3-3d-2	29
I.12	Test Data for Specimen B8-D-4-3d-1	30
I.13	Test Data for Specimen B8-D-4-3d-2	30
I.14	Test Data for Specimen B9-D-2-3d-2	30
I.15	Test Data for Specimen B10-D-4-7d-1	31
I.16	Test Data for Specimen B10-D-4-5d-1	31
I.17	Test Data for Specimen B11-D-3-7d-1	32
I.18	Test Data for Specimen B11-D-3-5d-1	32
I.19	Test Data for Specimen B12-D-2-7d-1	32
I.20	Test Data for Specimen B12-D-2-5d-1	33
I.21	Test Data for Specimen B1-SC-4-3d-1	33
I.22	Test Data for Specimen B1-SC-3-3d-1	33
I.23	Test Data for Specimen B1-SC-4-3d-2	33
I.24	Test Data for Specimen B3-SC-2-3d-1	33
I.25	Test Data for Specimen B4-SC-4-3d-1	34
I.26	Test Data for Specimen B4-SC-4-3d-2	34

I.27	Test Data for Specimen B5-SC-2-3d-2	34
I.28	Test Data for Specimen B6-SC-3-3d-1	35
I.29	Test Data for Specimen B6-SC-3-3d-2	35
I.30	Test Data for Specimen B7-SC-3-3d-1	35
I.31	Test Data for Specimen B7-SC-3-3d-2	35
I.32	Test Data for Specimen B8-SC-4-3d-1	36
I.33	Test Data for Specimen B8-SC-4-3d-2	36
I.34	Test Data for Specimen B9-SC-2-3d-1	36
I.35	Test Data for Specimen B9-SC-2-3d-2	36
I.36	Test Data for Specimen B10-SC-4-5d-1	37
I.37	Test Data for Specimen B11-SC-3-7d-1	37
I.38	Test Data for Specimen B11-SC-3-5d-1	38
I.39	Test Data for Specimen B12-SC-2-5d-1	38
I.40	Test Data for Specimen B4-P-4-3d-1	38
I.41	Test Data for Specimen B4-P-4-3d-2	38
I.42	Test Data for Specimen B6-P-3-3d-1	38
I.43	Test Data for Specimen B10-P-4-7d-1	39
I.44	Test Data for Specimen B10-P-4-5d-1	39
I.45	Test Data for Specimen B11-P-3-7d-1	39

INTRODUCTION

1.1 GENERAL BACKGROUND

Conventional concrete structures are reinforced with non-pre-stressed and pre-stressed steel. The steel is initially protected against corrosion by alkalinity of the concrete, usually resulting in durable and serviceable construction. For many structures subjected to aggressive environments, such as marine structures and bridges and parking garages exposed to deicing salts, combinations of moisture, temperature, and chlorides reduce the alkalinity of the concrete and result in corrosion of reinforcing and pre-stressing steel. To address corrosion problem, alternative metallic reinforcements such as epoxy coated steel bars are being used. While effective in some situations, such remedies may still be unable to completely eliminate the problems of steel corrosion (Keesler and Powers 1988).

Recently, composite materials made of fibers embedded in a polymeric resin, also known as fiber reinforced polymers (FRP), have become an alternative to steel reinforcement for concrete structures. As FRP are non magnetic and non corrosive, therefore, problems of electromagnetic interference and steel corrosion can be avoided with FRP reinforcement.

The development of FRP reinforcement can be traced to the expanded use of composites after World War II. The aerospace industry had long recognized the advantages of the high strength and light weight of composite materials. Due to problems of corrosion in important structures epoxy coated steel reinforcement appeared to be the best solution. The FRP reinforcement was not considered a viable solution or commercially available until the late 1970s in USA (ACI 440.1R-01).

Marshal-Vega Corporation led the initial development of glass fiber reinforced polymers (GFRP) reinforcing bars in the United States. Initially, GFRP bars were considered a viable alternative to steel as reinforcement for polymer concrete due to the incompatibility of the coefficients of thermal expansion

between polymer concrete and steel (ACI 440.1R-01).

The 1980s market demanded nonmetallic reinforcement for specific advanced technology. The largest demand for electrically nonconductive reinforcement was in facilities for magnetic resonant imaging (MRI) medical equipment. Other uses began to develop as advantages of FRP reinforcing became better known and desired, specifically in seawall construction, sub-station reactor bases, airport runways, and electronics laboratories (Brown and Bartholomew 1996).

In recent years, demand for steel has increased enormously due to the rapid growth and development in the Asian countries. This increase in steel demand has resulted in a steep rise in the prices of steel. Many countries of the region like Pakistan, are looking for cheap alternative materials. FRPs being lighter and stronger than steel can become a viable alternative.

1.2 PROBLEM STATEMENT

For reinforced concrete structures, the transfer of stresses between the concrete and the reinforcement, both at serviceability and ultimate load, is strongly dependent on the quality of bond. In fact, resisting mechanism under bending, shear and torsion are related to the development of adequate bond between concrete and reinforcement. Therefore, the development of adequate bond is always a critical aspect of the structural behavior, regardless of the type of reinforcement. Since the behavior of FRP reinforcement is quite different from steel reinforcement (Cosenza et al. 2001). Therefore, a better understanding of bond behavior is needed.

1.3 SCOPE

The scope of the study is to evaluate the bond behavior and effect of surface texture of plain, helically wrapped deformed, and sand coated GFRP rebars (#4, #3, and #2) in reinforced concrete (27.6 MPa, 34.5 MPa, and 41.4 MPa), using direct pullout test method.

1.4 OBJECTIVES

The main objectives of the research are:

- To study the behavior of bond slip and bond failure in GFRP rebars.
- To investigate the influence of embedment length on bond behavior of GFRP rebars.
- To investigate the effect of surface texture on bond behavior of GFRP rebars.
- To investigate the effect of concrete strength on bond behavior of GFRP rebars.

LITERATURE REVIEW

2.1 GENERAL

The earliest FRP materials used glass fibers embedded in polymeric resins that were made available by the burgeoning petrochemical industry following World War II. The combination of high-strength, high-stiffness structural fibers with low-cost, lightweight, environmentally resistant polymers resulted in composite materials with mechanical properties and durability better than either of the constituents alone. Fiber materials with higher strength, higher stiffness, and lower density, such as boron, carbon, and aramid, were commercialized to meet the higher performance challenges of space exploration and air travel in the 1960s and 1970s. At first, composites made with these higher performing fibers were too expensive to make much impact beyond niche applications in the aerospace and defense industries. The work to lower the cost of high performance FRPs started in the 1970s, especially to promote its substantial marketing opportunities in sporting goods (Bakis et al. 2002).

By the late 1980s and early 1990s, as the defense market waned, increased importance was placed by fiber and FRP manufacturers on cost reduction for the continued growth of the FRP industry. As the cost of FRP materials continues to decrease and the need for aggressive infrastructure renewal becomes increasingly evident in the developed world, pressure has mounted for the use of these new materials to meet higher public expectations in terms of infrastructure functionality. Aided by the growth in research and demonstration projects funded by industries and governments around the world during the late 1980s and throughout the 1990s, FRP materials are now finding wider acceptance in the characteristically conservative infrastructure construction industry (Bakis et al. 2002).

2.2 GFRP MATERIAL

2.2.1 Properties of GFRP Rebars

GFRP rebars are available in nominal diameters similar to those of steel rebars, however, they differ from steel rebars in two important aspects. First, GFRP rebars cannot be used as a substitute on a one-to-one basis for steel rebars, since their tensile strength and modulus of elasticity are different. The stress-strain behavior of GFRP rebars has a fairly linear relationship at all stress levels up to the point of failure, without exhibiting the yielding characteristic of steel (Larralde and Silva-Rodriguez 1993).

The tensile strength of the GFRP rebars is equal to and in some cases, depending on the glass content, greater than the yield stress of grade 40 and grade 60 steel rebars. The tensile modulus of elasticity is generally lower than that of steel. The deformation patterns on the surface of GFRP rebars are different from those of steel rebars (Larralde and Silva-Rodriguez 1993).

2.2.2 GFRP Manufacturing Process

The manufacturing method of choice, for both product consistency and economy, for structural shapes, is the pultrusion process. This continuous manufacturing process, which is highly automated, consists of “pulling” resin impregnated reinforcing fibers and fiber fabrics through a heated curing die. The common fiber reinforcement in pultruded shapes consists of fiber bundles (called roving for glass fiber and tows for carbon fiber), continuous strand mat (also called continuous filament mat), and non woven surfacing veils. In recent years, bidirectional and multidirectional woven, braided, and stitched fiber fabrics have been used to produce pultruded parts with enhanced mechanical properties (Bakis et al. 2002).

2.3 FRP BOND BEHAVIOR

When anchoring a reinforcing bar in concrete, the bond force can be transferred by:

- Adhesion resistance of the interface, also known as chemical bond.
- Frictional resistance of the interface.

- Mechanical interlock due to irregularity of the interface.

In FRP bars, it is believed that bond force is transferred through the resin to the reinforcement fibers, and a bond shear failure in the resin is also possible. When a bonded deformed bar is subjected to increasing tension, the adhesion between the bar and the surrounding concrete breaks down, and deformations on the surface of the bar cause inclined contact forces between the bar and the surrounding concrete. The stress at the surface of the bar resulting from the force component in the direction of the bar can be considered the bond stress between the bar and the concrete. Unlike reinforcing steel, the bond of FRP rebars appears not to be significantly influenced by the concrete compressive strength provided adequate concrete cover exists to prevent longitudinal splitting. (Nanni et al. 1995; Benmokrane, Tighiouart, and Chaallal 1996; Kachlakev and Lundy 1998)

2.3.1 Comparison of Steel and GFRP Bond Behavior

Anchorage design for steel rebars is not directly applicable on GFRP rebars. For the same test conditions, the average nominal bond stress at failure was greater for the steel rebars than for the GFRP rebars (Larralde and Silva-Rodriguez 1993). The bond strength of GFRP rebar is, on average, 40–100 per cent the bond strength on a steel rebar for pullout failure mode (Okelo and Yuan 2005). The damage during pullout of the steel rebars was solely located in the concrete, whereas in the case of GFRP rebars the damage was induced mainly to the rod or both to the rod and concrete (Katz 2000; Cosenza et al. 2001). The modulus of elasticity and the stiffness of the steel rebar are much higher than those of the concrete or the FRP rebars (210 GPa compared with 30–50 GPa for the concrete and GFRP) (Katz 2000). A reduction of between 80 and 90 per cent in the bond strength was found in case of GFRP rebars in comparison to a reduction of only 38 per cent in case of steel rebars in the same temperature range (Bank et al. 1999).

2.3.2 Influence of Embedment Length on Bond Strength

As long as the adhesive bond does not break embedment length has little effect on the bond strength, but when the adhesive bond breaks, and the GFRP rebar mechanically anchors to surrounding concrete, then the bond strength is

sensitive to embedment length and the bond strength decreases with increase in embedment length (Ehsani et al. 1996). Okelo and Yuan (2005), Achillides and Pilakoutas 2004, Zhang et al. (2002), and Larralde and Silva-Rodriguez (1993) have observed that reduction in bond strength is due to the nonlinear distribution of bond stress along the embedded length.

2.3.3 Influence of Compressive Strength on Bond Strength

Concrete with compressive strengths lower than 30 MPa, effect bond strength of GFRP rebars. As the concrete compressive strength is increased above 30 MPa, bond failure occur due to damage in the GFRP rebar and becomes independent of the concrete strength.

Okelo and Yuan (2005) carried out bond behavior study on GFRP rebars, with concrete compressive strength below 30 MPa, and found that the bond strength of the GFRP rebars is dictated by the shear strength of the concrete surrounding the GFRP rebar.

Achillides and Pilakoutas (2004) conducted study on GFRP bond behavior with concrete strengths greater than 30 MPa. They found that failure occurred on the surface of GFRP rebar. They observed that bond strength of GFRP rebars was not controlled by concrete strength but appeared to be influenced by the inter-laminar shear strength just below the resin rich surface layer of the GFRP rebar.

2.3.4 Influence of FRP Rebar Diameter on Bond Strength

The average bond strength of FRP rebars decreases as the reinforcing bar diameter is increased (Okelo and Yuan 2005).

Poisson effect, and shear lag are responsible for the phenomenon of decrease in bond strength due to increase in GFRP rebar diameter (Achillides and Pilakoutas 2004).

2.3.5 Influence of Surface Texture on Bond Strength

Surface texture has great influence on the bond strength of GFRP rebars. Deformed GFRP rebars perform better than plain GFRP rebars. Fig 2.1 shows GFRP rebars with different surface textures.

Katz (2000) studied bond behavior FRP rebars with different mechanical deformations and found that the FRP rebars with surface deformations performed well with an average bond stress ranging from 14.6 to 12.2 MPa.

Presence of deformations on the surface of FRP rebars plays a significant role on bond behavior because plain bars appeared to develop only 10–20% of the bond stress compared to deformed FRP rebars (Achillides and Pilakoutas 2004).



Fig. 2.1. GFRP bars of various diameters and surface types

EXPERIMENTAL INVESTIGATION

3.1 GENERAL

Pullout tests are widely adopted, as they offer an economical and simple solution for the evaluation of the bond performance of reinforcing bars and represent in a simple manner the concept of anchoring a bar (Cairns and Abdullah 1995). The main aim of pullout tests in this research is to obtain the bond-slip relationship at the loaded and free ends of GFRP rebars. The test data is used to ascertain bond behavior of GFRP rebars manufactured in Pakistan.

3.2 ESTABLISHMENT OF VARIABLES

To investigate bond behavior of GFRP rebars, concrete strength, rebar size, type of rebar surface texture, and embedment length are selected as variables.

3.3 MATERIAL PROPERTIES

Properties of the materials used in this research are summarized as follows:

3.3.1 Concrete Properties

Concrete mix was designed as per procedure prescribed by ACI 211.1-89. Twelve batches of concrete were prepared to cast seventy two specimens. Two cubes per batch are prepared for concrete compressive strength test. The specimens were prepared using concrete having three different compressive strengths which were 27.6 MPa, 34.5 MPa and 41.4 MPa. The results of 28 days cube compressive strength are tabulated in Table 3.1.

Table 3.1. Compressive Strength of Concrete Cubes at 28 Days

Batch number	Cube number	Load (KN)	Cube compressive strength (MPa)
B-1	1	670	29.33
	2	650	
B-2	1	630	28.89
	2	670	
B-3	1	630	29.33
	2	690	
B-4	1	870	37.78
	2	830	
B-5	1	890	38.67
	2	850	
B-6	1	910	39.78
	2	880	
B-7	1	950	42.67
	2	970	
B-8	1	1060	46.22
	2	1020	
B-9	1	1100	44.34
	2	1000	
B-10	1	1100	46.22
	2	980	
B-11	1	980	44.22
	2	1010	
B-12	1	1030	44.22
	2	960	

3.3.2 Glass Fiber Reinforced Polymer (GFRP) Reinforcing Bar Properties

GFRP rebars used in this study are manufactured by Fiber Craft Industries, Harbanspura, Lahore, Pakistan. These GFRP rebars are manufactured by means of pultrusion production process. In the tests presented herein, plain, deformed and sand coated bars are used. GFRP rebars of sizes, #2, #3, and #4 are used in this study. Detail of the GFRP rebars is tabulated in Table 3.2.

Table 3.2. Types of Bars Used in Pullout Tests

Bar Number	Type of bar	Surface texture	Bar diameter (mm)	Cross – sectional area (mm ²)
#4	GFRP plain	Smooth	12.0	113
#4	GFRP deformed	Medium rough	10.5	87
#4	GFRP sand coated	Rough	13.5	143
#3	GFRP plain	Smooth	9.5	71
#3	GFRP deformed	Medium rough	9.5	71
#3	GFRP sand coated	Rough	10.8	92
#2	GFRP plain	Smooth	6.0	28
#2	GFRP deformed	Medium rough	6.0	28
#2	GFRP sand coated	Rough	7.8	47

An experimental evaluation of mechanical properties was carried out by performing tensile tests, which are conducted using a universal load testing machine. For avoiding gripping problems due to the low transverse strength of the reinforcing bars, a gripping system based on embedding both ends of the GFRP rebar into a metal tube was adopted, and the bond between the GFRP rebar and the steel tubes was assured by an adhesive chemical commercially known as SIKAdur30.

3.4 SPECIMEN DESIGNATION

Seventy two specimens were tested to evaluate the bond behavior of GFRP rebar to concrete. The GFRP rebar tested were of three different sizes i.e. #2, #3, and #4 with three types of surface finish i.e. plain (P), deformed (D) and sand coated (SC). These bars were cast in twelve batches of concretes with three different cube compressive strengths i.e. 27.6 MPa, 34.5 MPa and 41.4 MPa. Two samples for each bar size, surface texture and embedment length were cast. The specimen designation symbols are tabulated in Table 3.3.

Table 3.3. Specimen Designation Symbols

Batch number	Surface texture			GFRP rebar size (mm)			Embedment length			Specimen number	
	Plain	Deformed	Sand coated	6.35	9.53	12.7	Terms of rebar diameter			1	2
B1-B12	P	D	SC	#2	#3	#4	3d	5d	7d		

The specimen designated as B1-P-2-3d-1, describes batch - B1, surface type - Plain, GFRP rebar size - #2, embedment length - 3 times bar diameter (#2), and specimen number 1.

3.5 PREPARATION AND CASTING OF SPECIMENS

The experimental process consisted of two parts i.e. casting and testing. Concrete cubes of 150 mm size were cast with GFRP bars placed vertically in the middle of cube. The embedment lengths were selected as multiples of the bar diameter to facilitate comparisons between GFRP rebars of different diameters. For the purpose of de-bonding the remaining rebar length inside the cube, PVC pipe of diameter larger than rebar size was inserted on the rebar and filled with wax.

The bar alignment jigs were constructed with laminated wooden boards and 13 mm diameter holes in the middle. PVC pipes of 150 mm length are inserted in the hole to grip the GFRP rebars vertically. Fig 3.1 illustrates GFRP rebars cast in concrete cube moulds where bar alignment jigs placed on top to ensure verticality of GFRP rebar.

The GFRP rebars were properly prepared and positioned vertically in the middle of the cube mould. Concrete was poured around the GFRP rebars. While concrete was still in plastic state, alignment jigs were placed on top of the moulds. The concrete cube moulds were opened 24 hours after casting and the specimens placed in curing tank for 28 days. The schedule of casting of specimens is tabulated in Table 3.4.



Fig. 3.1. GFRP rebars cast in concrete cubes with bar alignment jig.

Table 3.4. Schedule for Casting of Pullout Specimens

Batch number	Concrete strength (MPa)	Date of casting	Bar number	Number of bars			Development length
				P	D	SC	
B1	27.6	22/02/2006	#4, #3	2	2	2	3d
B2	27.6	22/02/2006	#4, #3	2	2	2	3d
B3	27.6	23/02/2006	#2	2	2	2	3d
B4	34.5	23/02/2006	#4	2	2	2	3d
B5	34.5	24/02/2006	#2	2	2	2	3d
B6	34.5	24/02/2006	#3	2	2	2	3d
B7	41.4	27/02/2006	#3	2	2	2	3d
B8	41.4	27/02/2006	#4	2	2	2	3d

Table 3.4. Continued

B9	41.4	28/02/2006	#2	2	2	2	3d
B10	41.4	28/02/2006	#4	2	2	2	5d & 7d
B11	41.4	1/3/2006	#3	2	2	2	5d & 7d
B12	41.4	1/3/2006	#2	2	2	2	5d & 7d

3.6 TESTING OF SPECIMENS

The concrete specimens prepared were tested in a universal testing machine (UTM). Schematic diagram of the pullout test procedure is shown in Fig. 3.2. For this purpose a complete testing rig was prepared.

The test rig consists of a 25 mm thick reaction plate with hole in middle and placed on top of the UTM moving head, a dial gauge attached on top of the concrete cube with its slider tip pressed against free end of GFRP rebar, an assembly securing 3 dial gauges at underside of UTM moving head with their slider tips pressed against a wooden plate attached to the GFRP rebar. The specimens are placed inverted on the reaction plate with GFRP rebar passing through the reaction plate and held in the lower grips of the UTM.

After securing the sample in the UTM, direct tension was applied to the GFRP rebar specimen, in deflection controlled mode. To take off readings, from the 3 bottom dial gauges, a digital video camera was set on stand with the bottom 3 gauges in view. Readings against load were noted on the top gauge and at the same time load value was shouted into the camera microphone. Later the video camera was played back on a monitor, pausing at every load shout to note down readings from the 3 dial gauges.

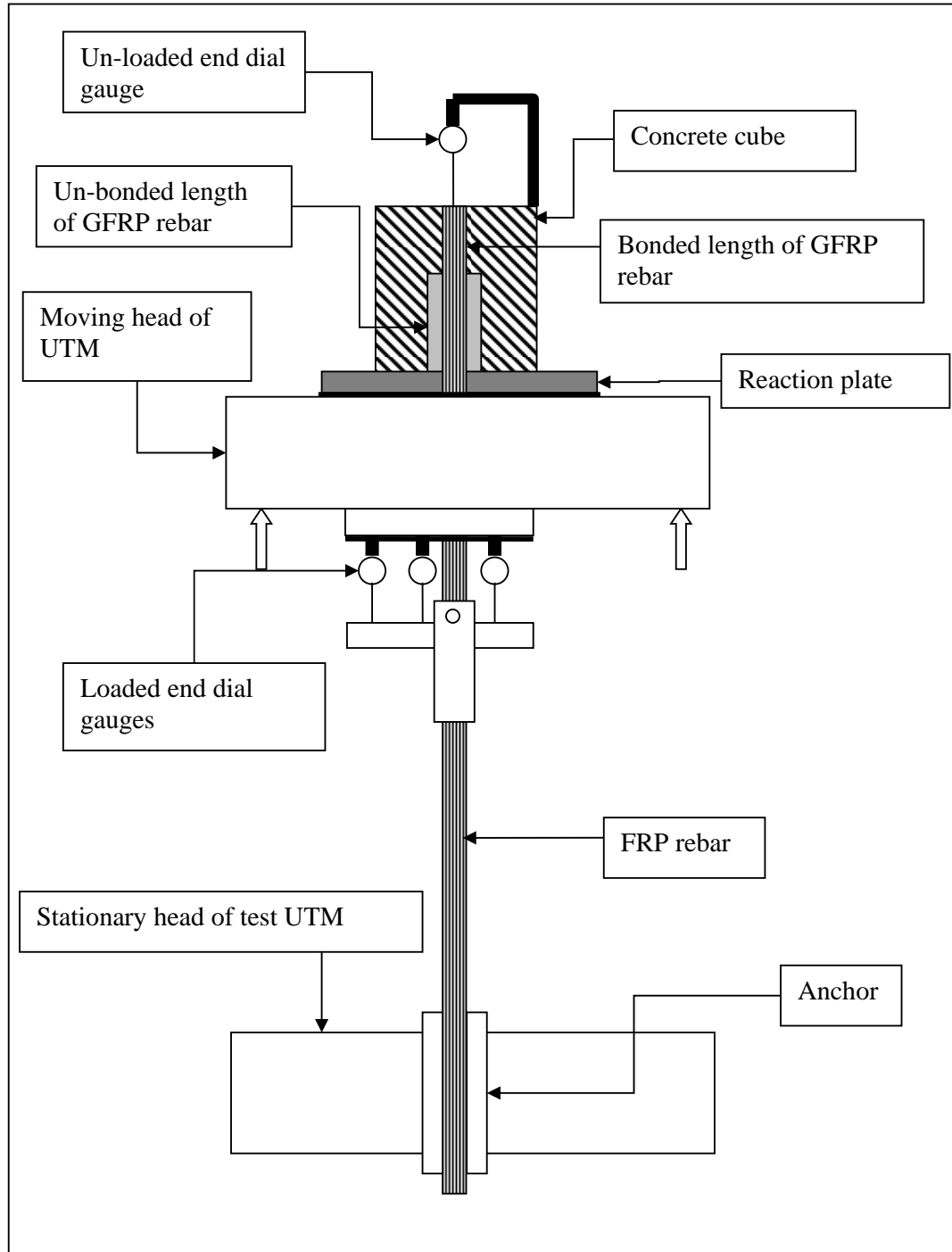


Fig. 3.2. Schematic details of pullout bond test

TEST RESULTS AND ANALYSIS

Tests are performed according to test arrangement explained in section 3.6. Direct tension is applied to the GFRP rebar. Readings are noted from the dial gauges at loaded and unloaded ends against load values. From load and dial gauge readings, bond stress versus slip curves are drawn for both loaded and unloaded ends of GFRP rebar. The bond stress versus slip curves for all specimens are graphically illustrated in Fig I.1 to I.44 (Appendix I). The load value at which unloaded end dial gauge shows a change in reading is called slip load and the corresponding reading of loaded end dial gauges is called slip. A summary of concrete compressive strength, embedment length, surface type, slip and slip load are summarized in Table I.1 (Appendix I) for all specimens. These results are analyzed to evaluate the bond behavior of GFRP rebars.

4.1 BOND STRESS VERSUS SLIP OF GFRP REBARS

Table I.1 (Appendix I) tabulates the slip load with the corresponding slip for 72 specimens. Readings were recorded for 44 out of the 72 specimens, as the rest of the specimens failed at low loads without showing any meaningful readings on the dial gauges at loaded and unloaded ends. Test data for these 44 specimens is tabulated in Table I.2 to I.45 (Appendix I), where applied load, bond stress, slip at loaded end, and slip at unloaded end are given. Bond stress versus slip curves for the specimens are graphically illustrated in Fig I.1 to I.44 (Appendix I). The following subsections discuss the bond versus slip behavior of plain, deformed and sand coated GFRP rebars:

4.1.1 Deformed GFRP Rebars

Bond stress versus slip results for deformed GFRP rebars are tabulated in Tables I.2 to I.20 and graphically illustrated in Fig I.1 to I.19 (Appendix I). During the tests it was observed that deformed GFRP rebars did not fail abruptly and

maximum bond stress developed is in the range of 4.0 to 11.0 MPa. Residual bond strength is observed in deformed GFRP rebars. Tests performed on deformed bars by Achillides and Pilakoutas (2004) found similar trend with maximum bond stress values ranging from 4.0 to 14.0 MPa.

The residual bond strength value is more than 75 per cent of the peak bond value in most of the specimens. Achillides and Pilakoutas (2004) have reported residual bond strength value of more than 60 per cent.

4.1.2 Sand Coated GFRP Rebars

Bond stress versus slip results for sand coated GFRP rebars are tabulated in Tables I.21 to I.39 and graphically illustrated in Fig. I.20 to Fig. I.38 (Appendix I). During the tests it was observed that sand coated GFRP rebars did not fail abruptly and maximum bond stress developed is in the range of 2.0 to 9.0 MPa. Residual bond strength is observed in sand coated GFRP rebars. The residual bond strength value is more than 60 per cent of the peak bond value in most of the specimens.

The bond strength of sand coated GFRP rebars are similar to that of deformed GFRP rebars. Similar trends are reported by Katz (2000).

4.1.3 Plain GFRP Rebars

Bond stress versus slip results for plain GFRP rebars are tabulated in Tables I.40 to I.45 and graphically illustrated in Fig. I.39 to Fig. I.44 (Appendix I). During the tests on plain GFRP rebars it was observed that the failure occurs abruptly and did not show residual bond strength. All plain GFRP rebars failed at bond stress values in the range of 0.7 to 2.0 MPa.

Tests performed on plain bars by Achillides and Pilakoutas (2004) found similar trend with failure bond stress values ranging from 0.1 to 1.3 MPa.

4.2 BOND FAILURE MODE OF GFRP REBARS

In the pullout tests, generally GFRP rebars bond failure occurred due to ripping / failure of GFRP rebar material at the surface (pull-through mode). Since no signs of splitting cracks appeared on the cube specimens, it is therefore assumed that concrete cubes provided adequate confinement to the GFRP rebars. However,

in case of concrete strengths more than 30 MPa, bond failure occurred partly due to peeling of the rebar surface and partly due to scraping of the surrounding concrete surface.

Fig. 4.1 and Fig.4.2 illustrates GFRP specimen samples after the test. The GFRP rebar is scratched, and tiny fibers are seen on the surface.

Fig 4.3 represents cross-section of a cube after test showing mode of bond failure of deformed GFRP rebar. Remains of crushed resin and chopped glass fiber in concrete are observed at the embedment location. Similar behavior is reported by Cosenza et al. (2001).



Fig. 4.1. Damage to the deformed GFRP bar after pullout

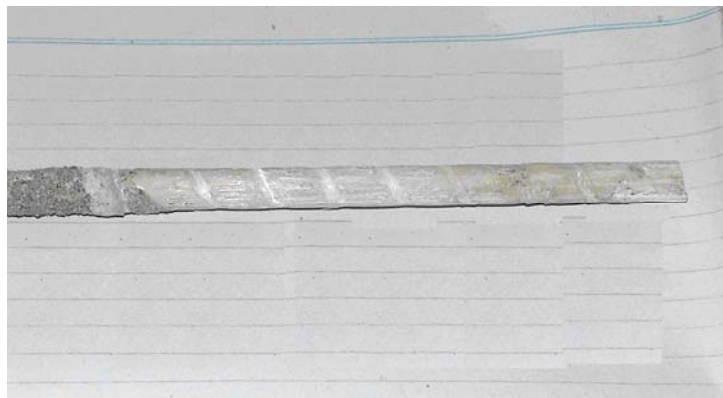


Fig. 4.2. Sand coated GFRP bar, sand coating completely peeled off after test



Fig. 4.3. Cross-section of concrete block showing crushed resin and chopped glass fiber remains

4.3 FACTORS INFLUENCING THE BOND BEHAVIOR OF GFRP REBARS

Factors influencing the bond behavior of GFRP rebars are analyzed as under:

4.3.1 Embedment Length

The maximum bond stress versus the embedment length for #4, #3 and #2 deformed rebars are shown in Fig. 4.4, Fig. 4.5, and Fig. 4.6. For #3 deformed GFRP rebar, the percentage decrease in bond stress is approximately 26 per cent, for increase in embedment length from 3d to 7d. Similar trends are observed in all tests of GFRP rebars. Larralde and Silva-Rodriguez (1993) have reported the similar trends, stating the reason, that this behavior could be the result of the nonlinear distribution of bond stress on the bar.

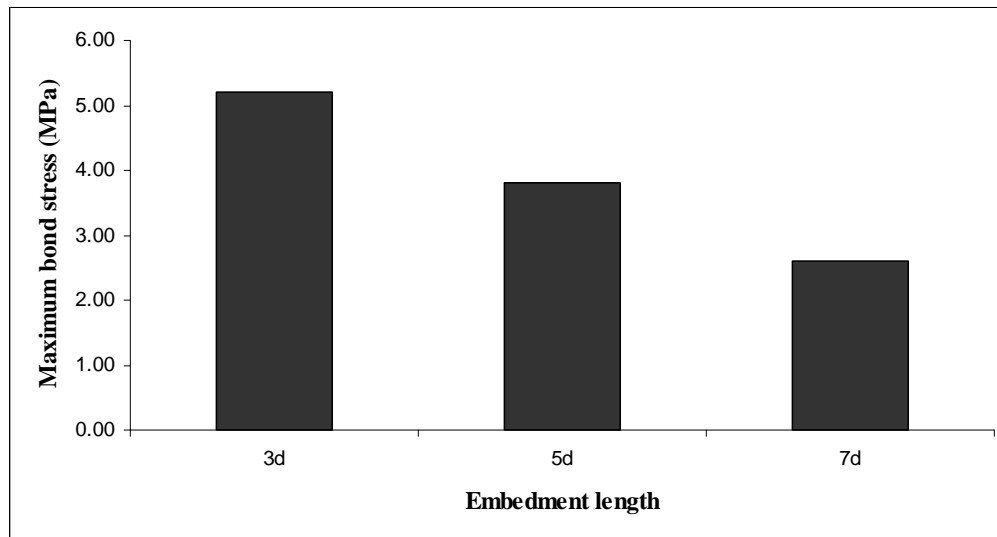


Fig. 4.4. Influence of embedment length on maximum bond stress for #4 deformed GFRP rebar

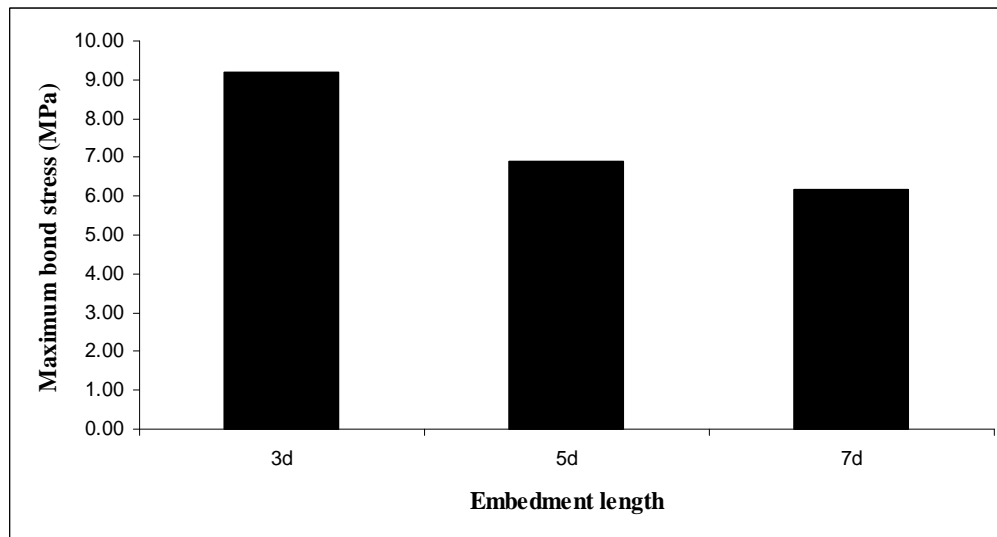


Fig. 4.5. Influence of embedment length on maximum bond stress for #3 deformed GFRP rebar

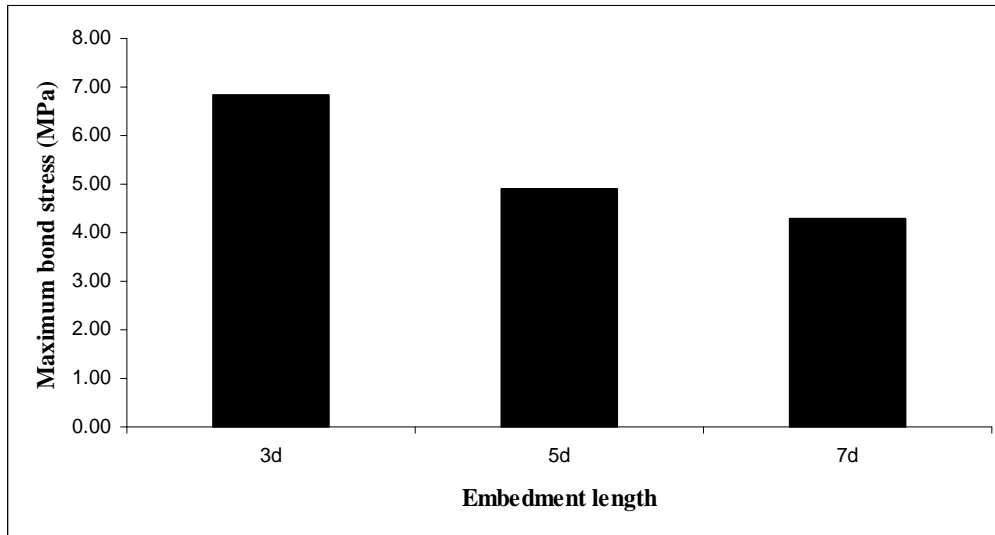


Fig. 4.6. Influence of embedment length on maximum bond stress for #2 deformed GFRP rebar

4.3.2 GFRP Rebar Size

Larger diameter rebar as shown in the Fig. 4.7 develop less average bond strength. The value of maximum bond stress of #2 deformed bar is 35 per cent higher than the #3 deformed bar at embedment length of 3d. Achillides and Pilakoutas (2004) considered Poisson effect, and shear lag to be responsible for lower bond strength with larger FRP rebar sizes.

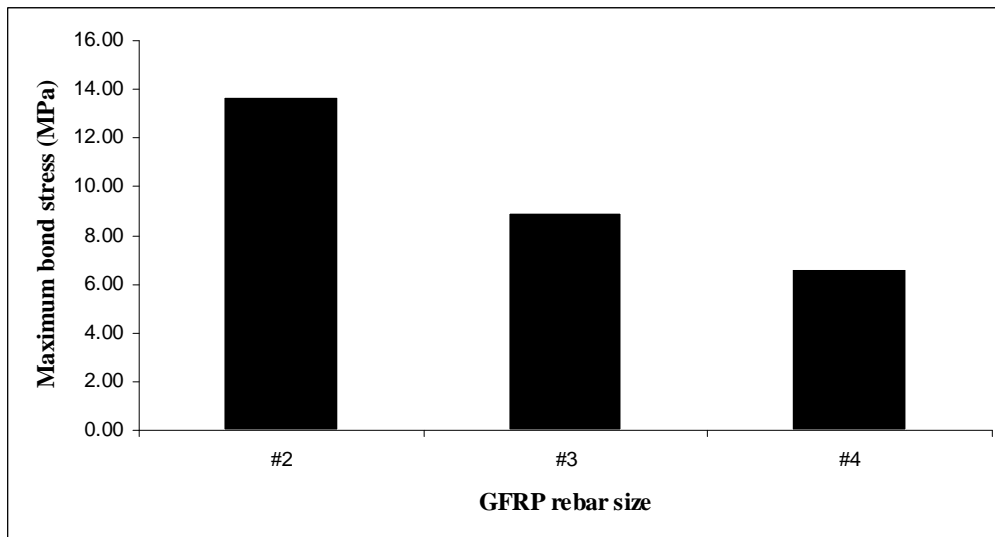


Fig. 4.7. Influence of rebar diameter on maximum bond stress

4.3.3 Surface Deformations

As illustrated in Fig. 4.8, the surface texture and deformations has significant effect on maximum bond stress. The analysis of test results indicate that for #4 bars with embedment length of 5d, the maximum bond stress is 0.96, 6.5, and 10.2 MPa for plain, sand coated and deformed GFRP rebars respectively. This indicates that the presence of deformations on the surface of GFRP bars play a significant role on bond behavior. Plain bars develop only 10 per cent bond stress compared to deformed bars of same diameter and embedment length. Similar trends are reported by Katz 2000 and Achillides and Pilakoutas 2004.

The bond strength of FRP rebars is assumed to depend mainly on mechanical interlock of surface deformations (Achillides and Pilakoutas 2004).

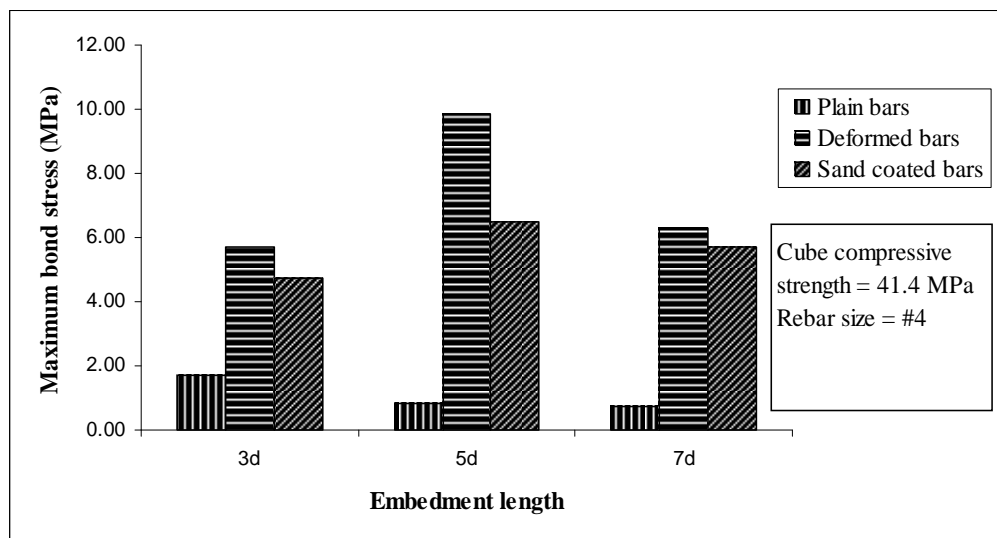


Fig. 4.8. Effect of surface texture, deformation, and embedment length on maximum bond stress

4.3.4 Concrete Strength

The test results indicate that the concrete strength below 34.5 MPa has significant effect on the bond strength. Fig. 4.9 graphically illustrates effect of concrete compressive strength on maximum bond stress of deformed GFRP rebar #3. Analysis of test data shows that for increase in concrete compressive strength from 34.5 to 41.4 MPa, the increase in maximum bond stress is only 14 per cent, which is not significant compared to the 275 per cent increase in maximum bond

stress when cube compressive strength increases from 27.6 MPa to 34.5 MPa. This means that concrete compressive strength has significant influence on bond strength of GFRP rebars at concrete strengths less than 34.5 MPa, whereas, at concrete strengths above 34.5 MPa the effect of concrete strength is not significant. Similar trends are reported by Achillides and Pilakoutas (2004).

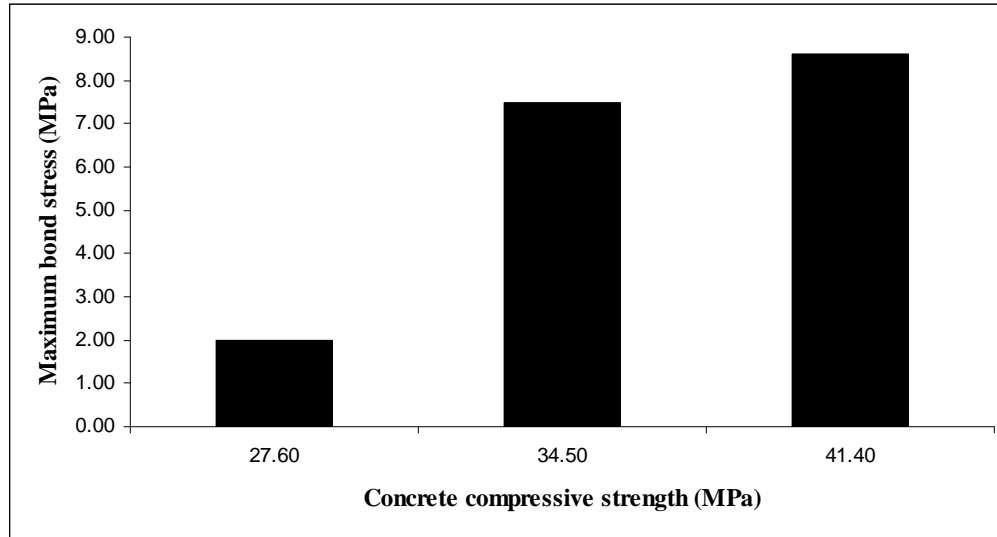


Fig. 4.9. Influence of concrete compressive strength on bond stress of #3 deformed rebars

CONCLUSIONS AND RECOMMENDATIONS

5.1 CONCLUSIONS

The test result analysis of direct pullout tests on GFRP rebars manufactured in Pakistan lead to following conclusions:

- Generally the specimens in pullout tests failed in a pull-through mode.
- Increase in the embedment length, decreases bond strength.
- Smaller diameter GFRP rebars develop higher bond strengths than larger diameter GFRP rebars.
- Deformed GFRP rebars performed better than plain and sand coated GFRP rebars in bond behavior.
- Plain GFRP rebars offer no mechanical interlock and have poor bond strength.
- Effect of concrete compressive strength, below 34.5 MPa has significant influence on bond strength, whereas, concrete compressive strength above 34.5 MPa has no significant influence on the bond strength of GFRP rebars.

5.2 RECOMMENDATIONS FOR FUTURE RESEARCH

- Pullout tests are used to investigate the bond behavior in this research, beam test may be used to investigate bond behavior in future studies.
- Since GFRP rebars develop bond by mechanical interlocking, which maybe improved by changing the deformation depths. Future research maybe focused on optimizing the deformation depths.

REFERENCES

- Achillides, Z., and Pilakoutas, K. (2004). "Bond behavior of fiber reinforced polymer bars under direct pullout conditions." *J. Compos. Constr.*, 8(2), 173-181.
- American Concrete Institute (ACI) (1989). "Standard practice for selecting proportions for normal, heavyweight, and mass concrete." *ACI 211.1-89*, Farmington Hills, MI.
- American Concrete Institute (ACI) (2001). "Guide for the design and construction of concrete reinforced with FRP bars." *ACI 440.1R-01*, Farmington Hills, MI.
- American Concrete Institute (ACI) (2004). "Guide for the design and construction of concrete reinforced with FRP bars." *ACI 440.3R-04*, Farmington Hills, MI.
- Bakis, C. E., Bank, L. C., and Brown, V. L., Cosenza; E., Davalos, J. F., Lesko; J. J., Machida; A., Rizkalla, S. H., and Triantafillou, T. C. (2002). "Fiber-reinforced polymer composites for construction—state-of-the-art review." *J. Compos. Constr.*, 6(2), 73-87.
- Benmokrane, B., Tighiouart, B., and Challal, O. (1996). "Bond strength and load distribution of composite GFRP reinforcing bars in concrete." *ACI. Mater. J.*, 93(3), 246-253.
- Bank, L. C., Berman, N., and Katz, A. (1999). "The effect of high temperature on bond properties of FRP rebars in concrete." *J. Compos. Constr.*, 3(2), 73-81.
- Brown, V., and Bartholomew, C. (1996). "Long-term deflections of GFRP reinforced concrete beams." *Proc., 1st Int. Conf. on compos. in infrastructure (ICCI-96)*, Tucson, Ariz., 389-400.
- Cairns, J. and Abdullah, R. (1995). "An evaluation of bond pullout tests and their relevance to structural performance." *Struct. Eng.*, 73(11), 179-185.
- Cosenza, E., Pecce; M., Manfredi, G., and Realfonzo, R. (2001). "Experimental and analytical evaluation of bond properties of GFRP bars." *J. Mater. Civ. Eng.*, 13(4), 282-290.

- Ehasani, M. R., Saadatmanesh, H., and Tao, S. (1996). "Design recommendations for bond of GFRP rebars to concrete." *J. Struc. Eng.*, 122(3), 247-254.
- Ehasani, M. R., Saadatmanesh, H., and Tao, S. (1997). "Bond behavior of deformed GFRP rebars." *J. Compos. Mater.*, 31(14), 1413-1430.
- Focacci, F., Nanni, A., and Bakis, E. C. (2000). "Local bond-slip relationship for FRP reinforcement in concrete." *J. Compos. Constr.*, 4(1), 24-31.
- Kachlakev, D. I., and Lundy, J. R. (1998). "Bond strength study of hollow composite rebars with different micro structures." *Proc., 2nd Int. Conf. on compos. in infrastructure (ICCI-98)*, Tucson, Ariz., 1-14.
- Katz, A. (2000). "Bond to concrete of FRP rebars after cyclic loading." *J. Compos. Constr.*, 4(3), 137-144.
- Keesler, R. J., and Powers, R. G., (1988). "Corrosion of epoxy coated rebars-keys segmental bridge-monroe county." *Rep. No. 88-8A*, Florida Department of Transportation, Materials Office, Corrosion Research Laboratories, Gainesville, Fla.
- Larralde, J., and Silva-Rodriguez, R. (1993). "Bond and slip of FRP rebars in concrete." *J. Mater. Civ. Eng.*, 5(1), 30-40.
- Meyer, R. W. (1985). *Handbook of pultrusion technology*, Chapman & Hall, London.
- Nanni, A., Bakis, C. E., and Boothby, T. E. (1995). "Test methods for FRP-concrete systems subjected to mechanical loads: state of the art review." *J. Reinforced plastics and Compos.*, Vol 9, 524-588.
- Okelo, R., and Yuan, R. L. (2005). "Bond strength of fiber reinforced polymer rebars in normal strength concrete." *J. Compos. Constr.*, 9(3), 203-213.
- Zhang, B., Benmokrane, B., and Gao, D. (2002). "Investigation of bond in concrete member with fiber reinforced polymer (FRP) bars." *J. Mater. Civ. Eng.*, 14(5), 399-408.